Development of multiscale hyperspectral sensing for integrated remote and proximal characterization of mineralized districts

Anna Sorrentino

Department of Earth, Environment and Resource Sciences, University of Napoli - Federico II, Via Cintia 26, 80126, Napoli
DOI: 10.19276/plinius.2025.01.018

INTRODUCTION AND AIMS

Since its advent, hyperspectral remote sensing has been widely used in Earth observation for various geological applications, enabling the detection and quantitative analysis of surface materials through calibrated reflectance spectra acquired as images in hundreds of narrow, contiguous spectral bands, typically within the Visible Near-Infrared (VNIR; 400–1300 nm) and Shortwave-Infrared (SWIR; 1300–2500 nm) regions (Bedini, 2017) (Fig. 1). Solar radiation interacting with an exposed surface causes absorption at specific wavelengths. The resulting reflectance spectra contain spectral signatures, or "fingerprints," that enable the identification of rock-forming minerals.

Notably, it has proven to be a powerful and cost-effective tool for mineral exploration of vast and remote areas, allowing the detection of hydrothermal and supergene alteration minerals, which serve as key vectors for identifying potential mineral deposits (Bedini & Chen, 2020).

Despite the widespread use of satellite- and airborne-based hyperspectral imaging for regional-scale exploration (*e.g.*, Laukamp et al., 2011; Sorrentino et al., 2024), close-range investigations using drones and tripod-mounted systems remain limited but crucial for understanding ore deposit formation and associated physicochemical gradients (Cudahy et al., 2008).

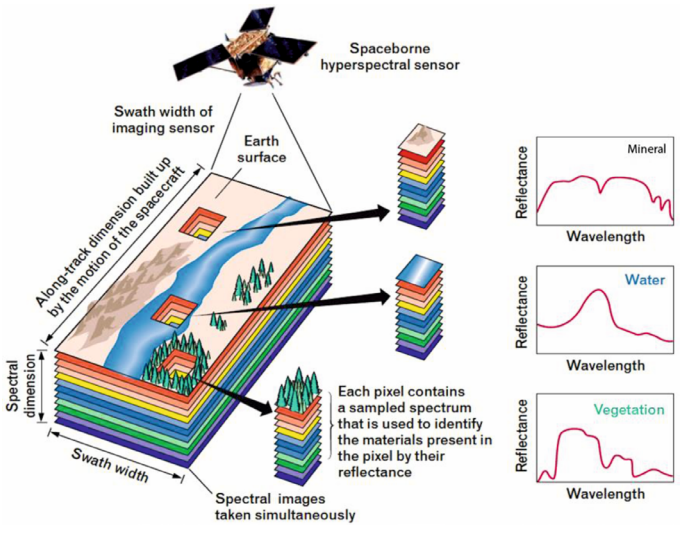

Figure 1 Schematic concept of hyperspectral sensing (from Bedini, 2017).

This PhD research aimed to bridge the scale gap by testing multi-scale hyperspectral sensing with new-generation satellite data, tripod-based imaging, and high-resolution sample-based point and imaging spectroscopy, across various mineralized areas worldwide, including porphyry-Cu and epithermal systems, Iron Oxide-Copper-Gold (IOCG) deposits, nonsulfide Zn mineralizations, and orogenic gold deposits (Fig. 2).

This approach enabled the detection and mapping of several ore-bearing and host-rock minerals, both well-documented phases (*e.g.*, Al-sheet silicates, alunite, carbonates; Laukamp et al., 2021) and previously un-characterized Zn-silicates.

VNIR-SWIR ABSORPTION FEATURES OF ROCK-FORMING MINERALS

Mineral species and groups exhibit diagnostic absorption features over the VNIR-SWIR spectral range (Clark et al., 1990; Laukmap et al., 2021).

In the VNIR region, absorption mainly results from electronic transitions of unfilled d-electron shells of transition metals and ligand-to-cation charge transfer, as observed in Fe-oxy-hydroxide minerals (Cudahy & Ramanaidou, 1997). In the SWIR range, vibrational modes dominate, due to bond stretching and bending in oxygen-bearing species, such as Al-OH in phyllosilicates, and C-O in carbonates (Laukamp et al., 2021).

The analysis of absorption features enables the estimation of key physicochemical properties of minerals, including: *i)* relative abundance, which is assumed to be proportional to the band depth (Clark et al., 1990); *ii)* chemical composition or mineral mixing, resulting in shifts in the wavelength position (Vedder & McDonald,

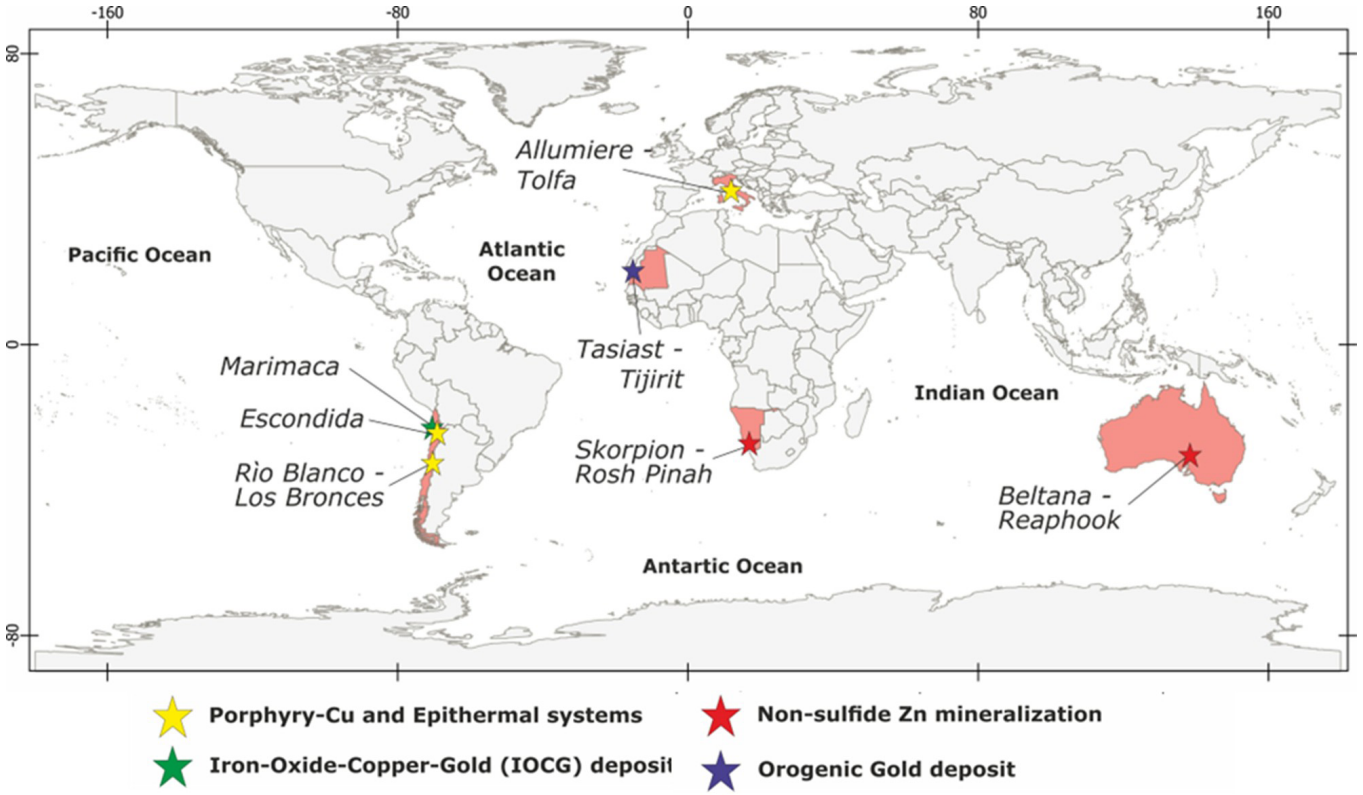

Figure 2 Global distribution of investigated study areas.

1963); *iii)* crystallinity degree, which decreases as the absorption width increases due to bond length variability in disordered structures (Murray & Lyons, 1955).

SPECTRAL MINERAL MAPPING AND HYPERSPECTRAL DATASET

In this thesis, spectral data were analyzed and processed to extract the previously mentioned spectral parameters and to identify VNIR-SWIR active minerals forming the investigated rocks. A multiple feature-guided workflow was employed, based on a combination of band ratios and minimum wavelength mapping methods.

The band ratio technique (Fig. 3a) involves constructing ratios to estimate relative abundance and chemical composition. For the former, it is calculated by dividing the sum of the shoulder reflectance values by that at the minima of a target absorption, while in the second case, it is calculated as the ratio between two specific bands (Laukamp et al., 2011). These analyses were performed using the Band Algebra Tool in ENVI software.

Minimum wavelength mapping (Fig. 3b) was instead employed using the open-source HyLite script in Python, as developed by Thiele et al. (2021). This method fits the absorption feature with a polynomial function of variable degree, within a specified range, allowing simultaneous extraction of all spectral parameters for each pixel.

At the regional scale, hyperspectral data were acquired from the Italian Space Agency's PRISMA and the German Aerospace Centre's EnMAP satellites, providing images of 30x30 km with a 30 m spatial resolution (for more specifics, see Chabrillat et al., 2024; Cogliati et al., 2021).

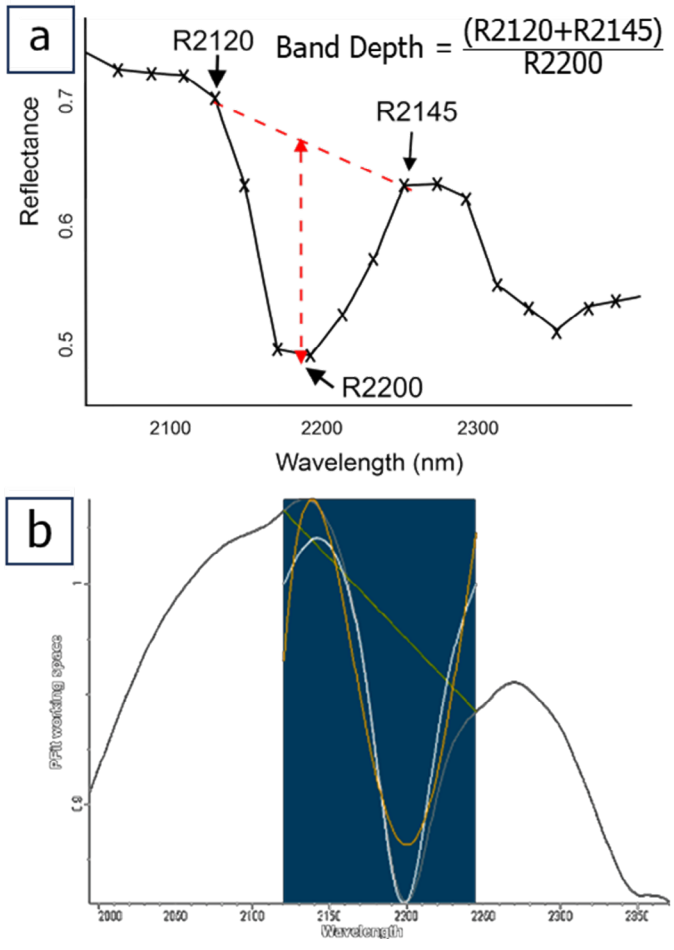

Figure 3 a) Band ratio and *b)* Minimum wavelength mapping methods (from CSIRO Mineral Resources).

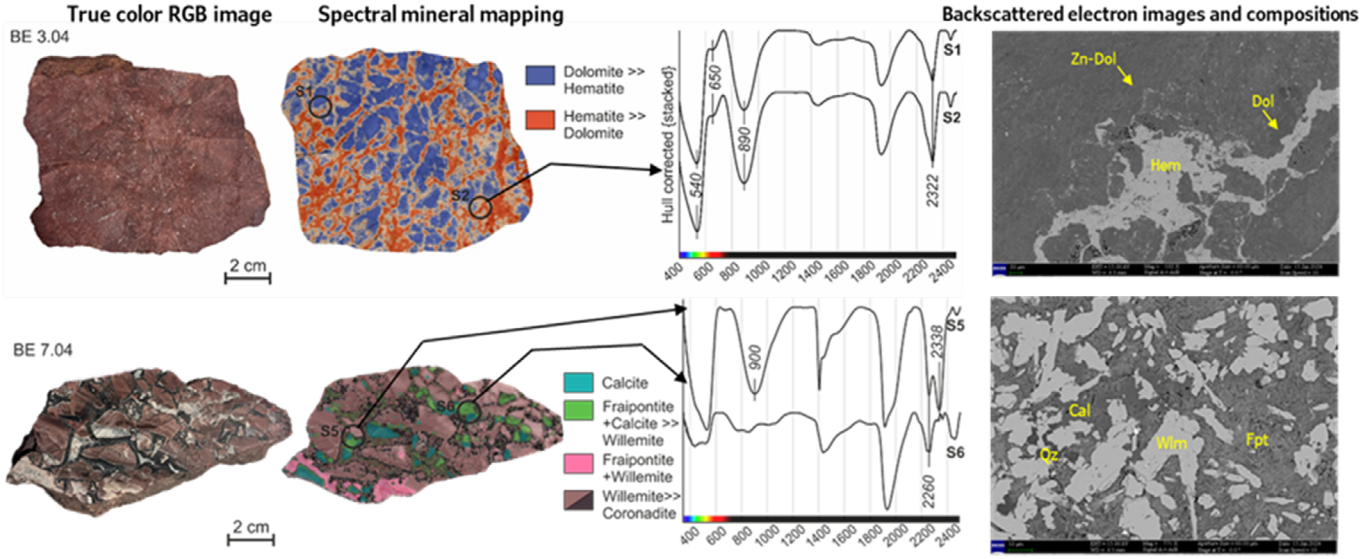

Figure 4 True-color and VNIR-SWIR hyperspectral images of altered and mineralized Beltana samples. Reflectance spectra from marked points are shown with the main absorption features. Backscattered electron images are depicted on the right.

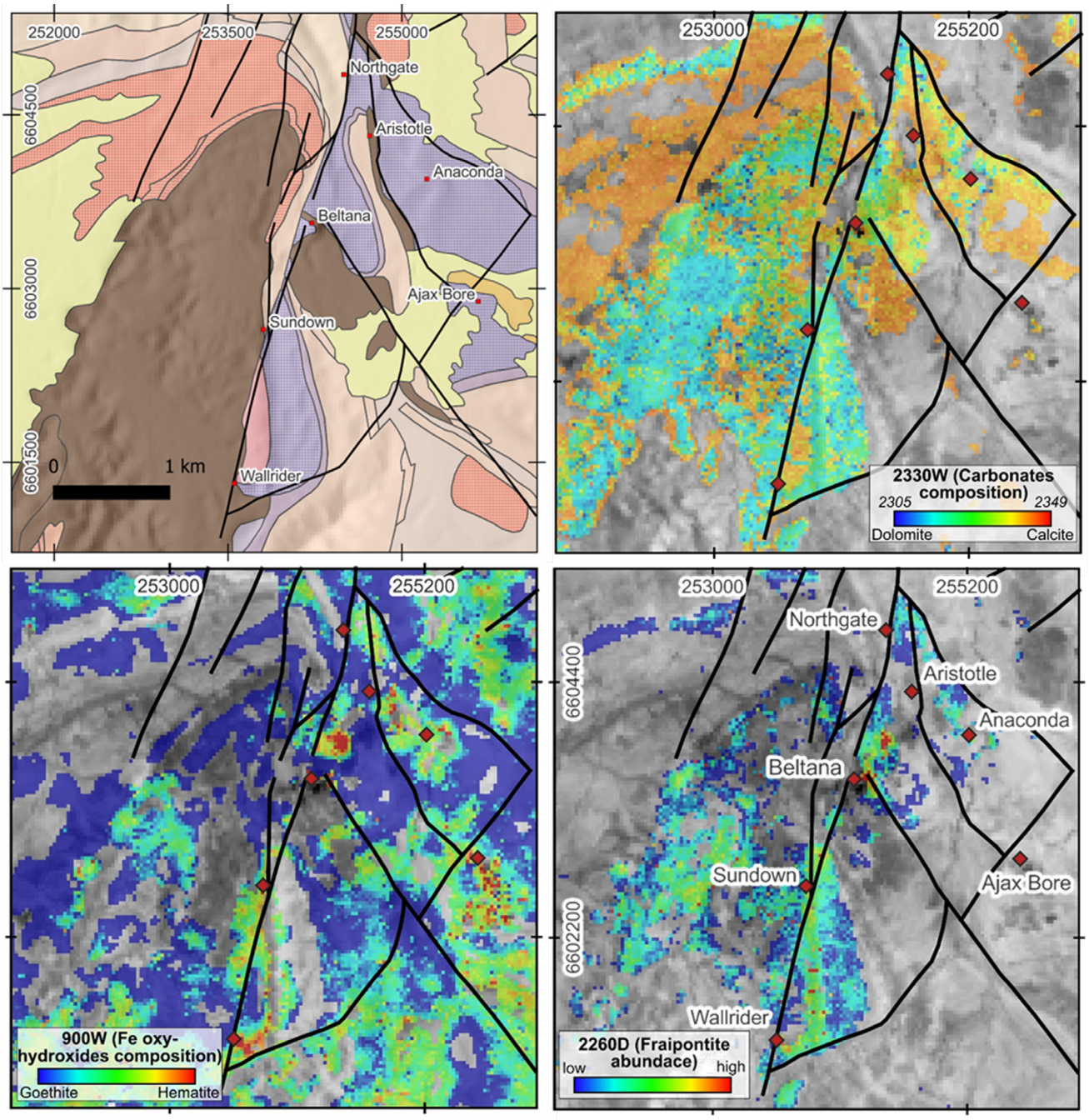

Figure 5 Geological map (from Groves et al., 2003) and EnMAP-derived spectral mineral products over the Beltana mining area.

At the outcrop and sample scales, hyperspectral data were collected using Headwall Photonics Micro- and Nano-Hyperspec cameras (supplied by the Department of Geosciences, University of Padua), mounted on tripods and in a laboratory setting. Moreover, high-resolution sample-based data were obtained at GFZ Potsdam with HySpex VNIR-1600 and SWIR-320m-e sensors, as well as the ASD FieldSpec-4 spectroradiometer.

The spectral results were further validated through mineralogical analyses on ground samples (*e.g.*, XRD, SEM, and optical microscopy).

MAIN RESULTS

Non-sulfide Zn mineralizations

The first case study is represented by the Beltana structurally-controlled Zn mineralized district located in the Flinders Ranges in South Australia. The Zn mineralization in this area is hosted by Lower Cambrian lithologies and contains significant willemite and fraipontite, associated with extensive hematite- and dolomite-bearing hydrothermal alteration (Groves et al., 2003).

Ten ground samples were analyzed through laboratory spectroscopy and mineralogical-petrographic methods (Fig. 4). Altered samples revealed the presence of hematite (absorption at ~870 nm) and dolomite (absorption at 2320 nm), which constitute the main pervasive alteration in the area. Spectral analyses of mineralized samples enabled the identification of spectral signatures of willemite (broad absorption feature between 900–1200 nm) and fraipontite (absorption at 2260 nm), previously unreported in the literature.

The same mineral phases were mapped at the regional scale using EnMAP satellite data (Fig. 5). Spectral mineral maps, representative of the relative abundance and chemical composition of alteration and ore minerals, were prepared by applying a multiple-feature extraction methodology based on polynomial fitting and band ratio.

The spectral products revealed the highest concentrations of fraipontite at the Beltana mining area, spatially associated with hematite and surrounded by dolomite. This also highlights the controlling effects of fault structures on mineralization and associated alteration haloes so that mineralized zones are punctually located at intersections between interacting faults or in the proximity of lateral fault terminations.

This work demonstrated the effectiveness of remote and proximal hyperspectral sensing for characterizing oxidized Zn mineralization, providing insights into the spectral behavior of several Zn-bearing minerals to support regional prospecting.

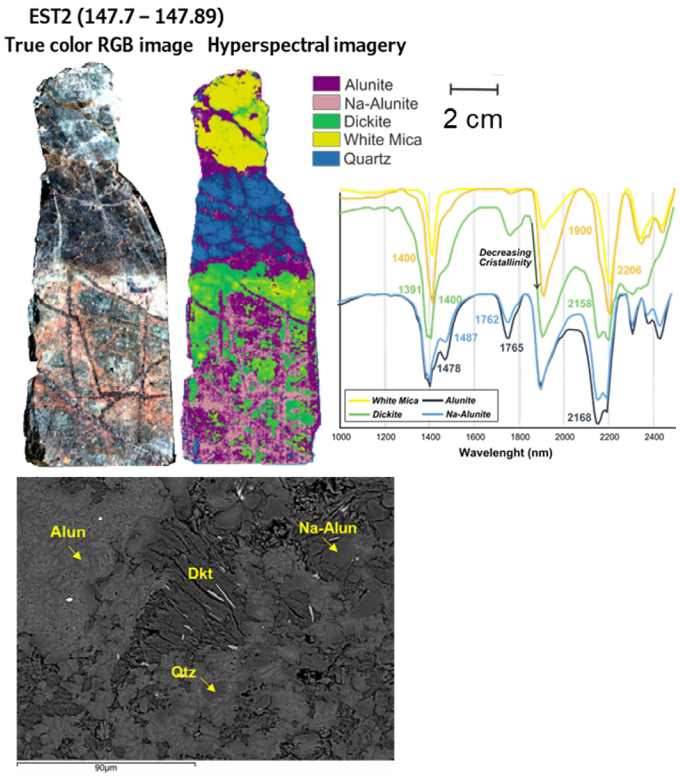

Figure 6 True-color and hyperspectral image of an Escondida sample. Reflectance spectra with the main absorption features are shown on the right. Backscattered electron images are reported at the bottom.

Porphyry copper deposits

The second case study is represented by the porphyry-Cu deposit of Escondida (Antofagasta Region, Northern Chile). The Escondida deposit, located in the Middle Eocene–Early Oligocene porphyry copper belt within the Domeyko Cordillera, hosts several orebodies centred on multiphase monzonitic-granodioritic-porphyry stocks (Hervé et al., 2012).

PRISMA and EnMAP satellite images were integrated with spectroscopic and mineralogical analyses (*i.e.*, optical and electron-scanning microscopy) conducted on forty-eight drill-core samples, to characterize the mineralogy of the wall-rocks in open pit areas.

Hyperspectral images of drill-core hyperspectral images were processed through the minimum wavelength mapping method, detecting several optically active mineral phases such as Fe oxy-hydroxides, chlorite and epidote, di-octahedral phyllosilicates (*i.e.*, white mica, pyrophyllite, kaolinite and dickite) and sulfates (*i.e.*, alunite, natroalunite, jarosite) minerals (Fig. 6).

At the district scale, the spatial distribution of alunite and kaolinite was mapped using the 2160 nm absorption feature in both PRISMA and EnMAP data. The PRISMA-derived map highlights higher concentrations in the eastern sector, with small spots in the northern and southern sectors. EnMAP results show a similar trend but outline a broader area in the northern sector (Fig. 7).

Notably, zones exhibiting higher concentrations of advanced argillic alteration minerals correspond to

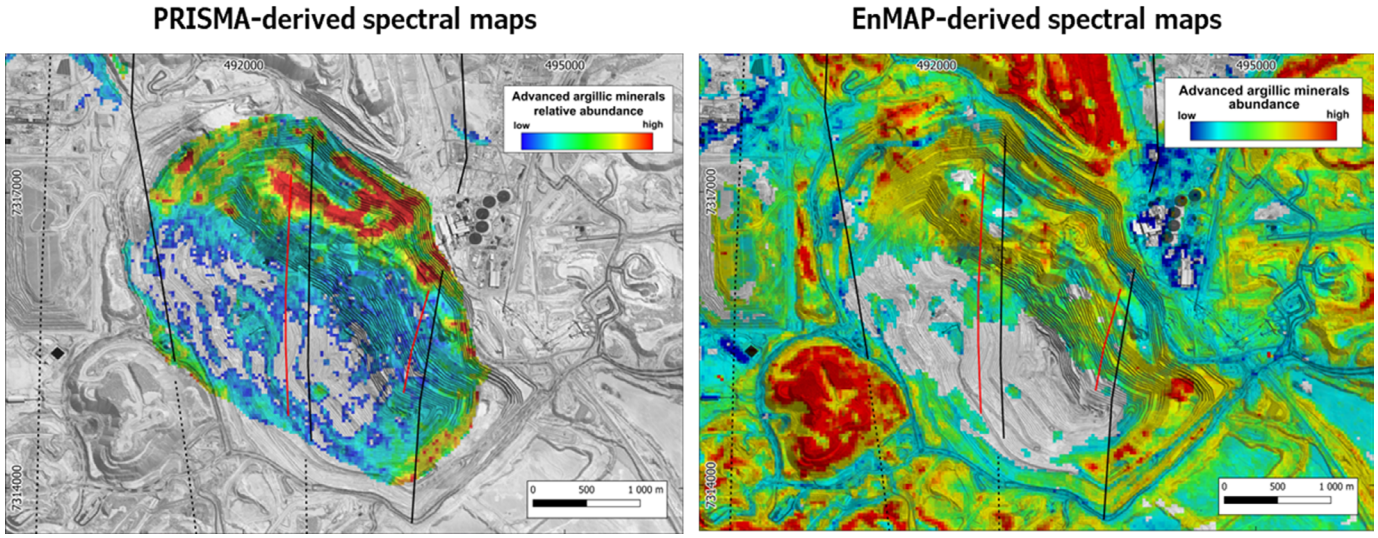

Figure 7 PRISMA- and EnMAP-derived mineral maps over the Escondida district.

domains of increased bench instability, consistent with sample-based observations.

The integration of multi-scale spectral data provides critical support for evaluating the bench stability across different domains of the pit. Moreover, these areas are progressively exposed due to ongoing exploitation processes, making this approach a rapid and cost-effective tool to be implemented along the mining value chain to provide real-time information on ore value and geotechnical evaluations.

High-sulfidation epithermal systems

As the third case study, the lithocap zone of the Allumiere epithermal system, north of Rome, was selected. The area is characterized by volcanic rocks, affected by widespread, structurally-controlled hydrothermal alteration, spanning from residual silica, to advanced argillic, to intermediate argillic zones, overprinted by supergene alteration (Marchesini et al., 2024).

Hyperspectral data were acquired at the Allumiere open pit mine, using tripod-mounted cameras and validated through laboratory imaging spectroscopy on 24 ground samples.

Mineral identification was performed using polynomial fitting and band ratios.

Sample-based analyses allowed to define the mineral assemblages associated with the distinct alteration zones typifying lithocap bodies, including sulfates (*i.e.*, alunite and natroalunite), kaolinite-group minerals (*i.e.*, kaolinite and dickite), Al- and Fe-rich smectites, opaline silica, and Fe-oxy-hydroxides (Fig. 8). These high-resolution data are crucial for defining outcrop-scale spectral targets and for cross-validation.

At the outcrop scale, hyperspectral images effectively mapped the relative abundances and compositional variations of these mineral phases (Fig. 9).

The spatial distribution of Fe oxides and hydroxides is likely associated with the presence of goethite, due to the Fe^{3+}- related absorptions (at ~ 900 nm). This mineral phase is rather widespread throughout the quarry, with the highest values predominantly concentrated

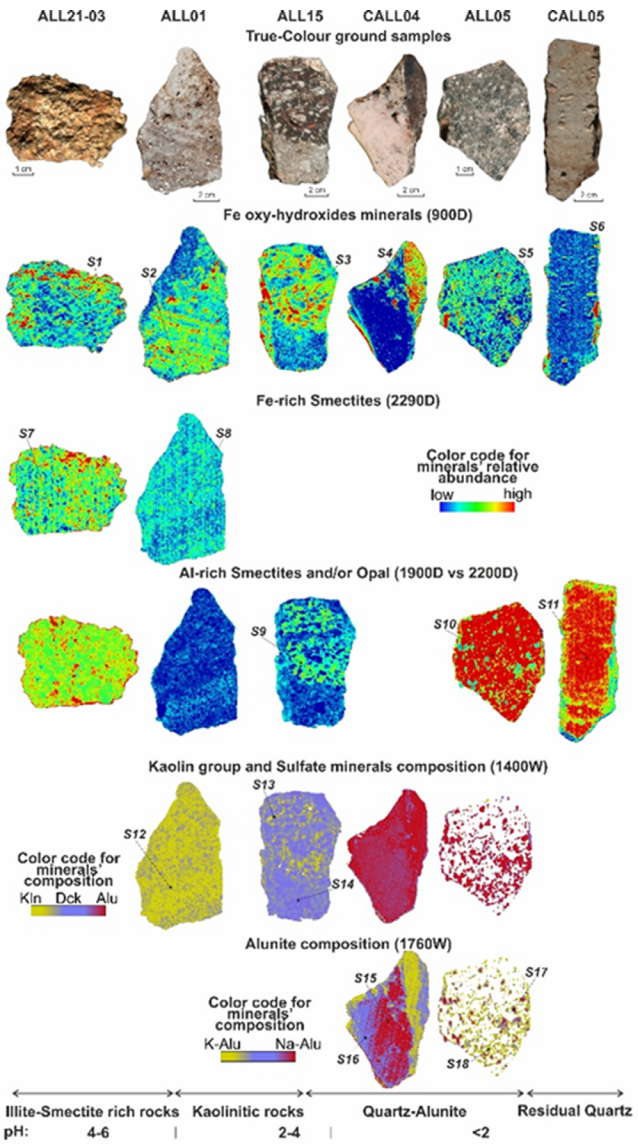

Figure 8 Hyperspectral imaging analysis conducted on six samples collected from the Allumiere quarry.

in the southeastern sector of the area, as well as in the uppermost benches.

Towards the southeastern sector, the high 900D values are coupled with medium to high relative abundances of the subtle feature at ~ 2290 nm, indicative of the presence of Fe-smectites. This portion of the quarry is also distinguished by deepest values of 2200D, which is mainly associated with the occurrence of Al-rich smectites and, to a lesser extent, opaline silica. The lowest values of this feature are found in the upper and inner part of the quarry, as well as towards the northwest in an area enclosed between faults.

The dominant mineral phases within the quarry, covering more than 80% of the area, consist of minerals belonging to the kaolin (*i.e.*, kaolinite and dickite) and sulfate groups, sharing the main absorption at ~ 2160 nm. These minerals display medium to high abundances, as highlighted by green to red colours, across the entire quarry area. Notably, the distribution of the highest values closely follows the trend of the main faults.

This approach provided significant insights into the geometry of the alteration mineral assemblages and their spatial relationship with the ore-controlling tectonic structures.

DISCUSSIONS AND CONCLUSIONS

This thesis demonstrates the potential of multi-scale hyperspectral imaging for ore deposit characterization. The research allowed developing advanced techniques for processing multi-scale spectral data. PRISMA and

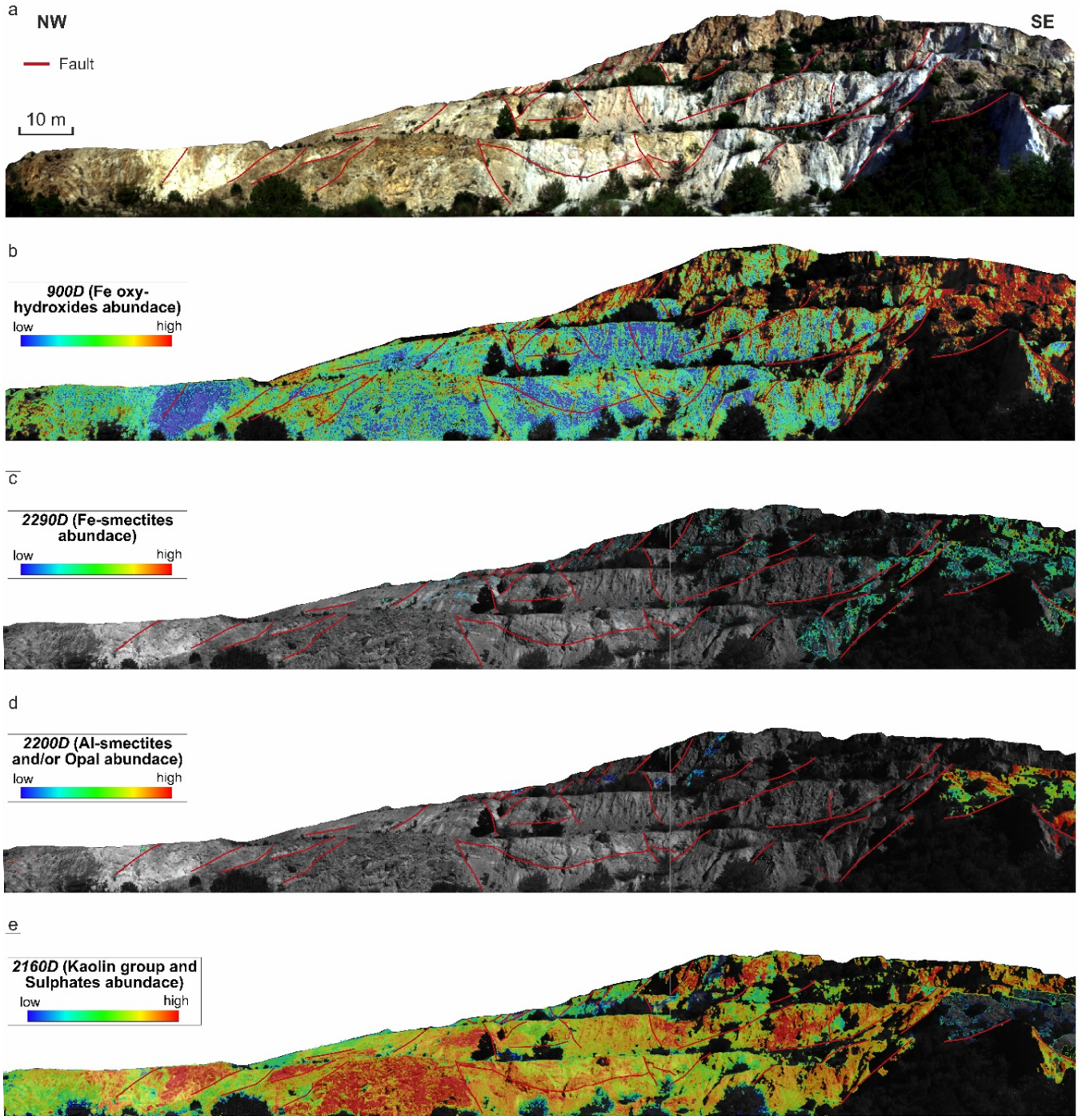

Figure 9 *Spectral mineral maps of the Allumiere quarry.*

EnMAP satellite data were integrated with high-resolution outcrop-scale scanning and image- and point-based analyses on samples. The adopted approach provided both a large-scale overview and detailed insights into the investigated mineralized areas.

Hyperspectral investigations, conducted across various geological settings, enabled the identification and detection of a wide range of mineral phases, such as Fe-oxy-hydroxides, phyllosilicates, sulfates, carbonates, and Zn-bearing minerals. The spectral data were successfully validated with common mineralogical analyses.

The feature extraction workflow based on band ratios and polynomial fitting allowed for a critical assessment of their advantages and limitations. The band ratio method is simple and fast, but less accurate for detecting subtle compositional variations (<10 nm spectral shift) or mineral mixing. Polynomial fitting is more precise but requires higher computational effort and careful parameter selection to avoid noise overfitting.

Overall, the results obtained highlight the effectiveness of integrating multiscale spectral datasets, enabling critical evaluations for exploration purposes with reduced costs and times, providing deposit-scale vectors toward mineralized centres to facilitate drilling, and supporting real-time ore evaluation and geotechnical assessment along the mining value chain.

REFERENCES

Bedini, E. (2017) - The use of hyperspectral remote sensing for mineral exploration: A review. J. Hyperspec. Remote Sens., 7, 4, 189–211.

Bedini, E. & Chen, J. (2020) - Application of PRISMA satellite hyperspectral imagery to mineral alteration mapping at Cuprite, Nevada, USA. J. Hyperspec. Remote Sens., 10, 2, 87–94.

Chabrillat, S., Foerster, S., Segl, K., Beamish, A., Brell, M., Asadzadeh, S., Milewski, R., Ward, K.J., Brosinsky, A., Koch, K. (2024) - The EnMAP spaceborne imaging spectroscopy mission: Initial scientific results two years after launch. Remote Sens. Environ., 114379.

Clark, R.N., King, T.V., Klejwa, M., Swayze, G.A., Vergo, N. (1990) - High spectral resolution reflectance spectroscopy of minerals. J. Geophys. Res-Solid Ea., 95, 8, 12653–12680.

Cogliati, S., Sarti, F., Chiarantini, L., Cosi, M., Lorusso, R., Lopinto, E., Miglietta, F., Genesio, L., Guanter, L., Damm, A. (2021) - The PRISMA imaging spectroscopy mission: Overview and first performance analysis. Remote Sens. Environ., 262, 112499.

Cudahy, T. & Ramanaidou, E. (1997) - Measurement of the hematite: goethite ratio using field visible and near-infrared reflectance spectrometry in channel iron deposits, Western Australia. Aust. J. Earth Sci., 44, 4, 411–420.

Cudahy, T., Jones, M., Thomas, M., Laukamp, C., Caccetta, M., Hewson, R., Rodger, A., Verrall, M. (2008) - Next generation mineral mapping: Queensland airborne HyMap and satellite ASTER surveys 2006–2008. CSIRO Report, 2007/364.

Groves, I.M., Carman, C.E., Dunlap, W.J. (2003) - Geology of the Beltana willemite deposit, Flinders Ranges, south Australia. Econ. Geol., 98, 4, 797–818.

Hervé, M., Sillitoe, R.H., Wong, C., Fernández, P., Crignola, F., Ipinza, M., Urzúa, F. (2012) - Geologic overview of the Escondida porphyry copper district, northern Chile. In: "Geology and Genesis of Major Copper Deposits and Districts of the World: A Tribute to Richard H. Sillitoe", J.W. Hedenquist, M. Harris, F. Camus, eds. Soc. Econ. Geol. Spec. P.

Laukamp, C., Cudahy, T., Thomas, M., Jones, M., Cleverley, J., Oliver, N. (2011) - Hydrothermal mineral alteration patterns in the Mount Isa Inlier revealed by airborne hyperspectral data, Aust. J. Earth Sci., 58, 8, 917–936.

Laukamp, C., Rodger, A., LeGras, M., Lampinen, H., Lau, I.C., Pejcic, B., Stromberg, J., Francis, N., Ramanaidou, E. (2021) - Mineral physicochemistry underlying feature-based extraction of mineral abundance and composition from shortwave, mid and thermal infrared reflectance spectra. Minerals, 11, 4, 347.

Marchesini, B., Tavani, S., Mercuri, M., Mondillo, N., Pizzati, M., Balsamo, F., Aldega, L., Carminati, E. (2024) - Structural control on the alteration and fluid flow in the lithocap of the Allumiere-Tolfa epithermal system. J. Struct. Geol., 179, 105035.

Murray, H.H. & Lyons, S.C. (1955) - Correlation of Paper-Coating Quality with Degree of Crystal Perfection of Kaolinite. Clay Clay Miner., 4, 31–40.

Sorrentino, A., Chirico, R., Corrado, F., Laukamp, C., Di Martire, D., Mondillo, N. (2024) - The application of PRISMA hyperspectral satellite imagery in the delineation of distinct hydrothermal alteration zones in the Chilean Andes: The Marimaca IOCG and the Río Blanco-Los Bronces Cu-Mo porphyry districts. Ore Geol. Rev., 105998.

Thiele, S.T., Lorenz, S., Kirsch, M., Acosta, I.C.C., Tusa, L., Herrmann, E., Möckel, R., Gloaguen, R. (2021) - Multi-scale, multi-sensor data integration for automated 3-D geological mapping. Ore Geol. Rev., 136, 104252.

Vedder, W. & McDonald, R.S. (1963) - Vibrations of the OH ions in muscovite. J. Chem. Phys., 38, 7, 1583–1590.